Journal of Hydroscience and Hydraulic Engineering
Vol. 10, No. 2, November, 1992, 13-25

TURBULENT OPEN-CHANNEL FLOW OVER BED COVERED BY RIGID VEGETATION

By

Tetsuro TSUJIMOTO

Associate Professor, Department of Civil Engineering, Kanazawa University
2-40-20, Kodatsuno, Kanazawa, 920, Japan

Yoshihiko SHIMIZU

Research Associate, Department of Civil Engineering, Gunma University
1-5-1, Tenjin-cho, Kiryu, 376, Japan

Tadanori KITAMURA

Research Assistant, Department of Civil Engineering, Kyoto University
Yoshida Honmachi, Sakyo-ku, Kyoto, 606, Japan

and

Toshiharu OKADA

Graduate Student, Department of Civil Engineering, Kanazawa University
2-40-20, Kodatsuno, Kanazawa, 920, Japan

ABSTRACT

Open channel flow over a rigid vegetation-covered bed was studied. The vegetation is simulated by cylinders of the same height and diameter set at equal spacings. Based on turbulence measurements in laboratory flumes with simulated vegetation, the turbulence structure of flow over the rigid vegetation-covered bed was investigated. Assuming similar Reynolds-stress profiles in the vegetation layer, the velocity profiles above and in the vegetation layer are described.

INTRODUCTION

Recent changes in approaches to river management require improvements in the hydraulics of flows with vegetation (see review paper by Tsujimoto (15)). One of the basic aspects is the turbulence characteristics of uniform flow over vegetabel covered beds, and this would provide information of velocity profiles, resistance law, and sediment transport. Previously, not the detail of turbulent structure but the Resistance law rather than details of turbulence structure has been used in investigations with classical approaches (Shen (12), Kouwen & Unny (5, 6, 7), Fukuoka & Fujita (3) and others). However, environmental aspects will need to be studied and with this more basic turbulence characteristics will contribute to the research.

The interactions between flow and vegetation differ for different species of water plants. When the vegetation layer over a bed is thin and the flow in the vegetation is negligible, the bed may be treated as a rough bed. But, when the vegetation layer is thicker and the flow inside the vegetation cannot be neglected, the interaction between the faster flow over the vegetation and the slower flow inside the vegetation must play an important role in the turbulence. This thicker vegetation case was investigated in this study. Three types of plants can be distinguished: (i) rigid plants; (ii) deformable (flexible) plants; and (iii) plants trailing along the bed. The investigation here is limited to (i).

The turbulence of air flow above and inside vegetation layers have been studied as "canopy flow" in meteorology and agricultural engineering (see the review paper by Thom & Raupach (14)), but little research has been reported for water flows except the pioneering work by Hino & Utahara (4) and work by Murota & Fukuhara (8, 9, 10) of turbulent flows with flexible plants ((ii) and (iii)).

In the study here, the vegetation is simulated by a group of cylinders of the same height and diameter set at equal spacings, and the turbulence characteristics of steady uniform flow over such a bed are investigated experimentally in a laboratory flume. Based on the experimental data, the classical turbulence model (mixing-length model) is modified by focussing on the interaction between the flows over and in the cylinders to describe the velocity profile from the flume bed to the water surface.

EXPERIMENTS OF FLOW OVER RIGID VEGETATION-COVERED BED

The flume experiments investigating turbulence characteristics of uniform flow over a rigid vegetation-covered bed have been conducted at Kanazawa (Series A) and Kyoto Universities (Series R) (Nakagawa et al. (11), Shimizu et al. (13), Tsujimoto & Kitamura (16)). The turbulent velocity was measured by a micro-propeller current-meter in Series A and by a hot-film anemometer in Series R.

The rigid (undeformable) cylinders of equal height (K) and diameter (D) were placed at equal spacings in a square pattern on smooth flume beds (see Table 1). The geometrical properties of a vegetation-layer model determine the characteristic velocity (u_s) in uniform flow when the flow depth is smaller than the vegetation height ($H<K$; H=flow depth measured from the bed to the free surface) and friction is negligible.

$$u_s = \sqrt{2gI/(C_D\lambda)} \tag{1}$$

where ρ=mass density of fluid; g=gravity acceleration, I=energy slope; C_D=drag coefficient; $\lambda \equiv D/s^2$=projected area of vegetation per unit volume of water in the flow direction. In this study, λ is so small that the net and the apparent velocities of flow in the vegetation layer can be considered equal. When $H>K$, and K sufficiently large, the velocity in the vegetation layer approximates this velocity far from the interface.

Table 1 Model vegetation in the flume experiments

Series	D (cm)	K (cm)	s (cm)	$\lambda \equiv D/s^2$ (cm^{-1})	equipped at
R	0.10	4.1	1.0	0.10	Kyoto University
A	0.15	4.6	2.0	0.0375	Kanazawa University

Table 2 Experimental conditions

RUN	H (cm)	h (cm)	I (10^{-3})	u_* (cm/s)	u_{*k} (cm/s)	U (cm/s)	h/K	i_b(10^{-3})
R21	6.36	2.26	0.96	2.45	1.46	6.52	0.55	0.66
R23	8.83	4.73	0.98	2.91	2.12	10.84	1.15	0.90
R25	10.54	6.44	1.15	3.20	2.69	14.68	1.57	0.99
R33	8.42	4.32	2.01	4.07	2.92	16.25	1.05	2.01
R34	9.41	5.31	1.83	4.11	3.09	18.19	1.30	1.83
R35	10.61	6.51	1.76	4.28	3.35	19.89	1.59	1.76
R41	6.59	2.39	4.70	5.51	3.32	14.52	0.58	2.33
R43	8.47	4.37	4.28	5.96	4.28	20.09	1.07	3.04
R60	3.77	--	3.20	3.44	--	10.48	--	3.20
A11	9.50	4.91	1.06	3.14	2.26	13.25	1.07	1.00
A12	7.49	2.90	1.42	3.23	2.01	11.72	0.63	1.00
A14	3.00	--	1.00	1.71	--	5.66	--	1.00
A31	9.36	4.77	2.60	4.88	3.48	19.59	1.04	3.00
A32	7.35	2.76	3.72	5.18	3.17	17.94	0.60	3.00
A34	3.07	--	3.00	3.00	--	10.38	--	3.00
A37	5.68	1.09	3.16	4.19	1.83	12.35	0.24	3.00
A71	8.95	4.36	8.86	8.82	6.15	33.05	0.95	7.00
A72	7.27	2.68	8.59	7.82	4.74	26.69	0.58	7.00
A74	3.94	--	7.00	5.20	--	16.66	--	7.00

The experimental conditions are summarized in Table 2: $h \equiv H\text{-}K$; $u_* \equiv \sqrt{\tau_0/\rho}$; $u_{*k} \equiv \sqrt{\tau_k/\rho}$; $\tau_0 = \rho g H I$=bed shear stress; $\tau_k \equiv \rho g h I$; I=energy gradient; i_b=bed slope; ρ=density of water; and U=depth averaged velocity.

EXPERIMENTAL RESULTS

Outline of the Results:

Some examples of profiles of velocities (u, measured at the center of 4 model plants), turbulence (u'_{rms}), and the Reynolds stress ($-\overline{u'v'}$) are shown in Figs.1~3, where y is the vertical distance from the interface between the surface-flow region and the vegetation layer, and the broken line indicates the interface.

When the depth is smaller than the vegetation height ($H<K$), there is a uniform velocity in the vegetation layer and the Reynolds stress is zero. The turbulence intensity is not zero but very small. When the depth is larger than the vegetation height ($H>K$), there is turbulent shear flow even in the vegetation layer suggesting an active momentum exchange there; the peak of the Reynolds stress is at the interface between the vegetation layer and the surface-flow region indicating that the flow is characterized by the shear at this level.

Figures 4 and 5 suggest the following approximations to the distributions of Reynolds stress and velocity in the vegetation layer ($-K<y<0$).

$$\tau_R(y) = \tau_k \exp \alpha y \qquad (-K<y<0) \qquad (2)$$

$$\frac{u-u_s}{u_k-u_s} = \exp \beta y \qquad (-K<y<0) \qquad (3)$$

with τ_R=Reynolds stress; τ_k=Reynolds stress at $y=0$ ($\tau_k = \rho g h I$; $h \equiv H\text{-}K$=surface flow thickness); α, β=constants; and u_k=velocity at $y=0$.

With a shear flow region in the vegetation layer, the force balance on a unit volume of water is written as:

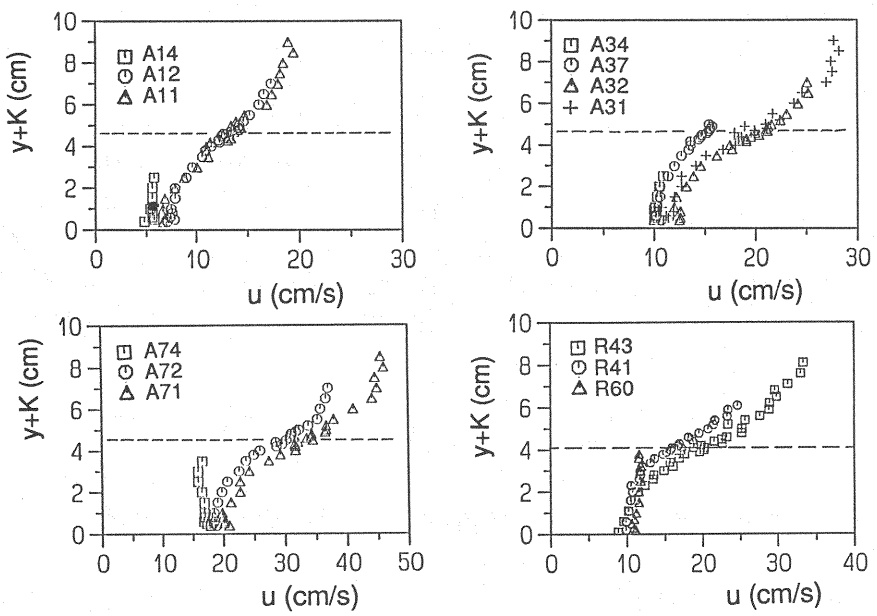

Fig.1 Velocity distribution above and inside vegetation layer

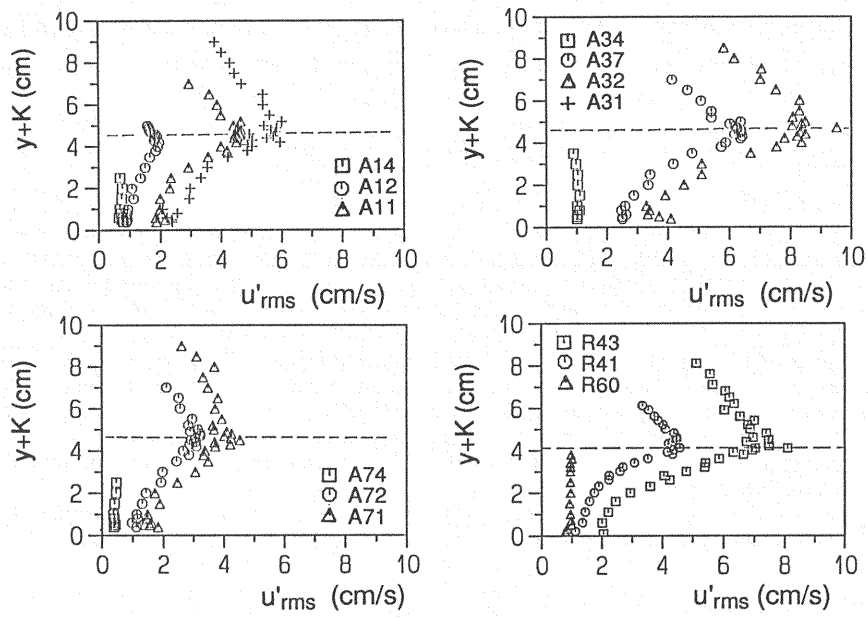

Fig.2 Distribution of turbulence above and inside vegetation layer

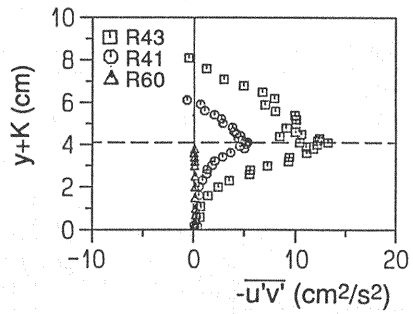

Fig.3 Distribution of Reynolds-stress of flow above and inside vegetation

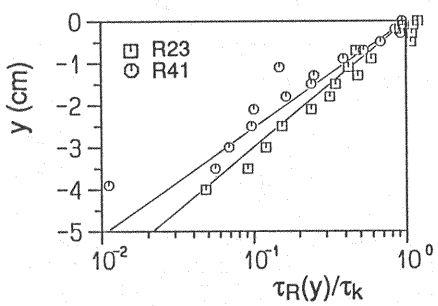

Fig.4 Reynolds-stress distribution in vegetation

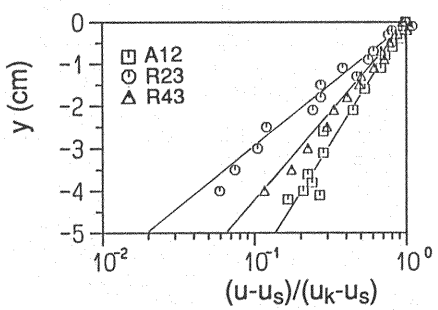

Fig.5 Velocity distribution in vegetation

$$\frac{d\tau_R}{dy} = -\rho g I + \frac{1}{2} C_D \rho u^2 \lambda \qquad (4)$$

This equation implies that, when $u(y)$ or $\tau_R(y)$ is known, the other can be deduced. Mathematically, however, exponential solutions of $\tau_R(y)$ and $u(y)$ cannot be deduced simultaneously from Eq.4, if one of $\tau_R(y)$ and $u(y)$ is assumed exponential, the other is not exponential but can be approximated by an exponential function.

The Reynolds-stress distribution in the surface-flow region peaks at the interface (see Fig.3) and

$$\tau_R(y) = \tau_k\left(1-\frac{y}{h}\right) \qquad (0<y<h) \qquad (5)$$

with $h\equiv H-K$. Then, the log-law is expected to remain valid in the surface-flow region.

Correction of Errors in Data of Energy Gradient:

In general, it is difficult to obtain accurate data of the energy slope in experiments. With the experimental characteristics above, data of the energy gradient can be properly corrected.

The accuracy of the measured velocity-profile is high, and Eq.3 may be adapted to the measured profile to determine β empirically, and, Eq.5 leads to the following distribution of Reynolds stress in the vegetation layer:

$$\tau_R(y) = -\rho g I(y-y_0)+\frac{(u_k-u_s)^2}{2\beta}\frac{\rho C_D\lambda}{2}\left(\exp 2\beta y - \exp 2\beta y_0\right)$$
$$+\frac{u_s(u_k-u_s)}{\beta}\frac{\rho C_D\lambda}{2}\left(\exp\beta y - \exp\beta y_0\right)+\frac{\rho C_D\lambda}{2}u_s^2(y-y_0) \qquad (-K<y<0) \qquad (6)$$

Integrating Eq.5 to obtain Eq.6, the boundary condition has been assumed as : $\tau_R=0$ at $y=y_0$ where y_0 is the height at which the velocity given by Eq.3 equals $u_s+0.1(u_k-u_s)$ ($y_0=-4.6/\beta$). The Reynolds stress produced by the shear of the bottom is neglected in Eq.5. At the bottom,

$$\tau_R(-0) = \frac{y_0}{H-K}\tau_R(+0) - \frac{(u_k-u_s)^2}{2\beta}\frac{\rho C_D\lambda}{2}\left(1 - \exp 2\beta y_0\right)$$
$$-\frac{u_s(u_k-u_s)}{\beta}\frac{\rho C_D\lambda}{2}\left(1 - \exp\beta y_0\right) - \frac{\rho C_D\lambda}{2}u_s^2 y_0 \qquad (7)$$

This calculation often shows a discontinuity of Reynolds stress at $y=0$, $\tau_R(-0)$ does not equal $\tau_R(+0)=\rho g h I$ with I as the measured energy slope. This discontinuity is mainly caused by errors in the measurement of I. Adjustment to the value of I brings changes to the values of u_s and successively that of β, Eq.6 leads to a revised Reynolds-stress distribution in the vegetation layer. This was repeated to minimize the discontinuity of the Reynolds stress at $y=0$, and the most reliable value of I was obtained.

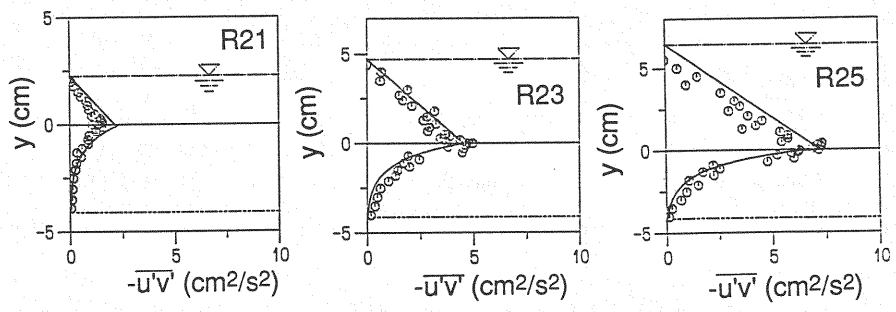

Fig.6 Reynolds-stress distribution for verification of energy-slope correction method

The correction procedure was tested with the data of Series R where the Reynolds-stress distribution was measured, and as shown in Fig.6, the calculated Reynolds-stress distribution is consistent with the measured one. Next, the procedure was applied to predict the Reynolds stress distribution in the vegetation layer from the measured velocity distribution when the Reynolds stress is not measured. Fig.7 shows the Reynolds-stress distribution predicted for Series A, and Fig.8 shows that the calculated Reynolds stress based on the assumption of Eq.3 is well approximated by an exponential function, though the calculated Reynolds-stress is smaller than the exponential approximation very deep in the vegetation layer.

The experimental conditions in Table 2 were corrected with this procedure.

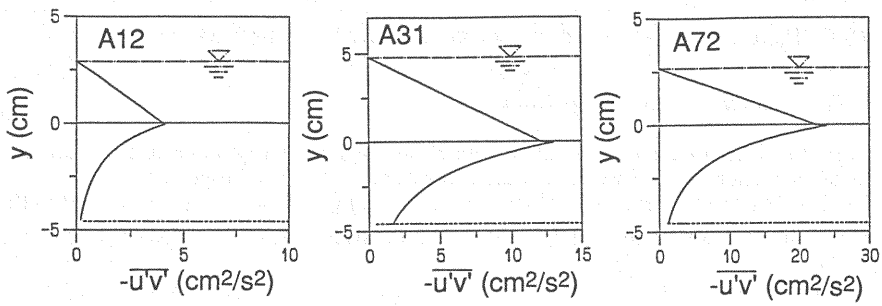

Fig.7 Estimated Reynolds-stress distribution for A series

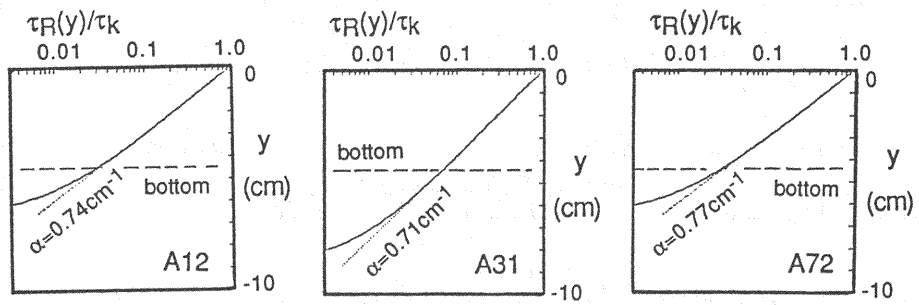

Fig.8 Comparison between Reynolds-stress distribution estimated from exponential velocity profile and exponential expression of Reynolds-stress distribution

Relations among Parameters to Determine Turbulent Structure:

The α, β, and u_k values obtained experimentally are shown in Figs.9 and 10. The plots of $\alpha\sqrt{sK}$ and $\beta\sqrt{sK}$ against hI/K scatter less than those of αs and βs. As α and β are reciprocals of length, they should be made dimensionless by the longitudinal and vertical lengths, s and K. The values of $\alpha\sqrt{sK}$ and $\beta\sqrt{sK}$ are similar and decrease slightly with hI/K. The u_k value is made dimensionless by the velocities, u_s and u_{*k}, and $(u_k-u_s)/\sqrt{u_s u_{*k}}$ are plotted against h/K with $u_{*k}\equiv\sqrt{\tau_k/\rho}$. Fig.10 suggests that $(u_k-u_s)/\sqrt{u_s u_{*k}}$ increases with h/K and becomes nearly constant for larger values of h/K.

Plots of $\alpha\sqrt{sK}$, $\beta\sqrt{sK}$, and $(u_k-u_s)/\sqrt{u_s u_{*k}}$ against hI/K or h/K are shown in Figs.9 and 10 where the corrected value of I is used (also in u_{*k}), they scatter less than the plots against hi_b/K or h/K where the value of I has been only poorly approximated by i_b (see Figs.11 and 12), and it supports the validity of the correction.

When both Eqs. 2 and 3 are valid, the distribution of mixing length in the vegetation layer is:

$$l(y)=\frac{u_{*k}}{\beta(u_k-u_s)}\exp\left[\left(\frac{\alpha}{2}-\beta\right)y\right] \qquad (-K<y<0) \qquad (8)$$

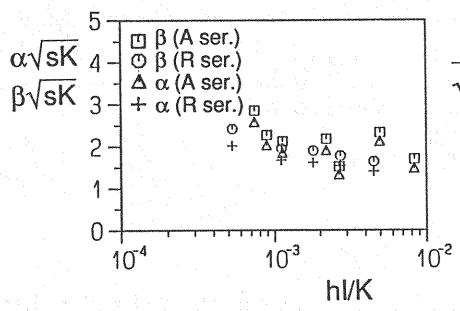

Fig.9 Relation between $\alpha\sqrt{sK}$, $\beta\sqrt{sK}$, and hl/K (after data correction for energy slope)

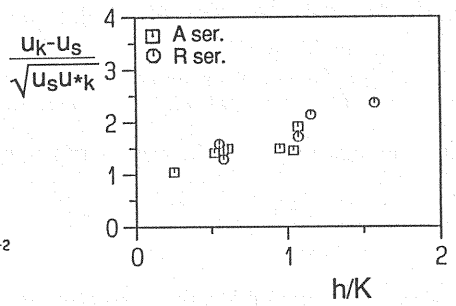

Fig.10 Relation between $(u_k-u_s)/\sqrt{u_s u_{*k}}$ and h/K (after data correction for energy slope)

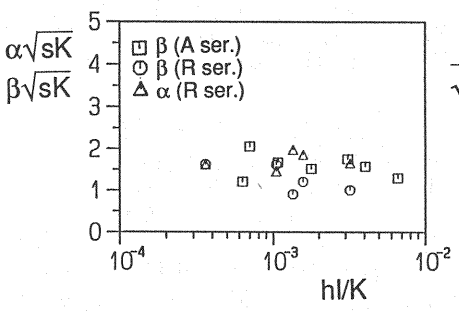

Fig.11 Relation between $\alpha\sqrt{sK}$, $\beta\sqrt{sK}$, and hl/K (before data correction for energy slope)

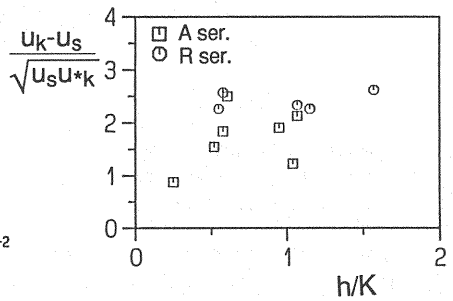

Fig.12 Relation between $(u_k-u_s)/\sqrt{u_s u_{*k}}$ and h/K (before data correction for energy slope)

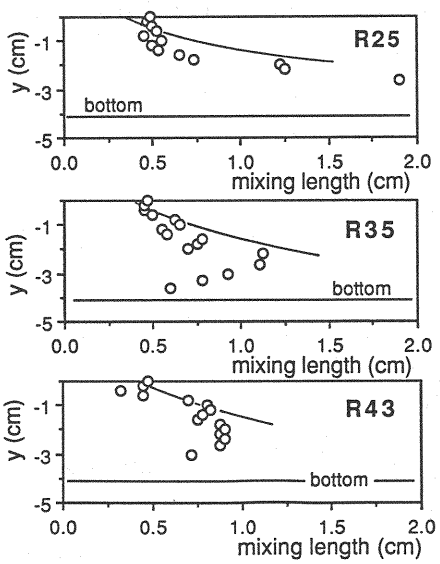

Fig.13 Mixing engths in vegetation layer

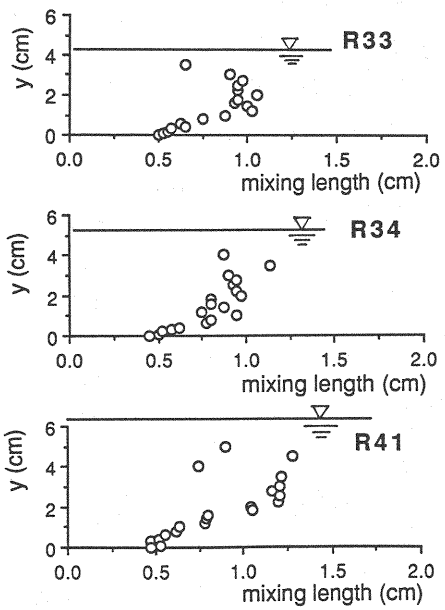

Fig.14 Mixing lengths above vegetation

This suggests that the mixing length increases with distance from the interface between vegetation and surface-flow as $\alpha<2\beta$ (see Fig.9), and this is experimentally confirmed in Fig.13. The data of the mixing length were obtained by spline-fitting of the measured profiles of velocity and Reynolds stress. This implies that the flow in the vegetation layer is subject to shear at the interface with the free-surface flow.

At the interface (y=0), Eq.8 gives the following non-zero mixing length:

$$l_0 \equiv l(0) = \frac{u_{*k}}{\beta(u_k - u_s)} \tag{9}$$

The non-zero mixing length at y=0 also affects the distribution of mixing length of free-surface flow. The mixing length of the free-surface flow reversely calculated from the measured velocity and Reynolds-stress distribution after spline fitting has a non-zero value at y=0 as shown in Fig.14 and it increases with the distance.

ANALYTICAL MODELLING OF TURBULENT STRUCTURE OF FLOW ABOVE AND INSIDE THE VEGETATION LAYER

Flow inside Vegetation Layer:

The Reynolds-stress in the vegetation layer is brought about by differences in the velocities between the faster surface flow and the slower flow in the vegetation. Mixing of momentum between the two layers may be caused by pressure fluctuations as pointed out by Chu & Gelhar (2) for seepage flow in highly permeable porous layers accompanying free-surface flow. The analytical results of Chu & Gelhar (2) suggests an exponential form of the Reynolds-stress profile induced in the vegetation layer. This allows Eq.3 rather than Eq.2 to be considered, suggesting that the parameter α must be determined. The interaction mechanism has not been analyzed, and the relation between $\alpha\sqrt{sK}$ and hI/K obtained by the experiments (Fig.9) can be empirically formulated as (see Fig.15):

$$\alpha\sqrt{sK} = -0.32 - 0.85 \cdot \log\left(\frac{hI}{K}\right) \tag{10}$$

Here hI/K is effective only when α is positive. The constants in the formula were determined by a least-squares method.

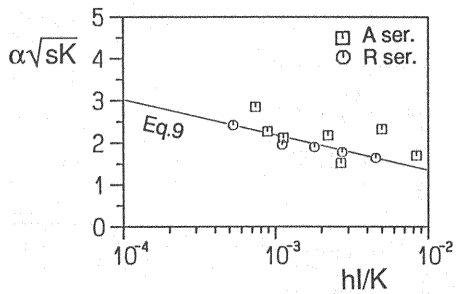

Fig.15 Relation between $\alpha\sqrt{sK}$ and hI/K

Assuming Eq.2, Eq.5 leads to the following velocity distribution in the vegetation layer.

$$u(y) = u_s \sqrt{1 + \frac{2\alpha}{C_D\lambda}\left(\frac{u_{*k}}{u_s}\right)^2 \exp\alpha y} = u_s \sqrt{1 + \alpha h \cdot \exp\alpha y} \tag{11}$$

Here Eq.1 and $u_{*k} \equiv \sqrt{ghI}$ have been substituted to obtain the final equation. The velocity at the interface between the surface-flow region and the vegetation layer, u_k, is written as:

$$u_k = u(0) = u_s \sqrt{1+\alpha h} \tag{12}$$

The values of u_k, calculated by Eq.12, are compared with the measured data in Fig.16(a), and this demonstrates that Eq.12 predicts u_k adequately. The relation between u_k/u_s and hI/K deduced from Eq.12 with Eq.10 is depicted with the data in Fig.16(b), where $\gamma \equiv h/\sqrt{sK}$.

The velocity profile calculated by Eq.10 can be approximated by an exponential function as shown in Fig.17. The exponential approximation is poor far from the interface. The solid curve in each figure represents Eq.11, while the chained curve is an exponential approximation obtained from the data by the least-squares method and the broken curve is an exponential function with gradient equal to the one given by Eq.11 at y=0. The parameter β of the third expression is determined by equating the velocity gradient at y=0 of Eq.11 with that of Eq.3. This gives the relation between β and α as:

$$\beta = \frac{\alpha}{2}\left(1+\frac{u_s}{u_k}\right) = \frac{\alpha}{2}\left(1+\frac{1}{\sqrt{1+\alpha h}}\right) \tag{13}$$

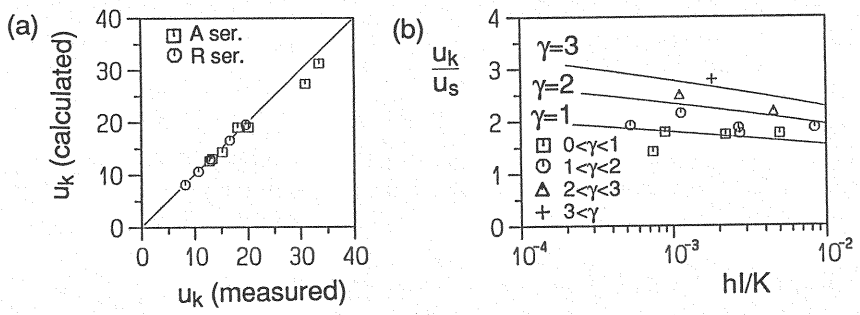

Fig.16 Verification of estimation of u_k

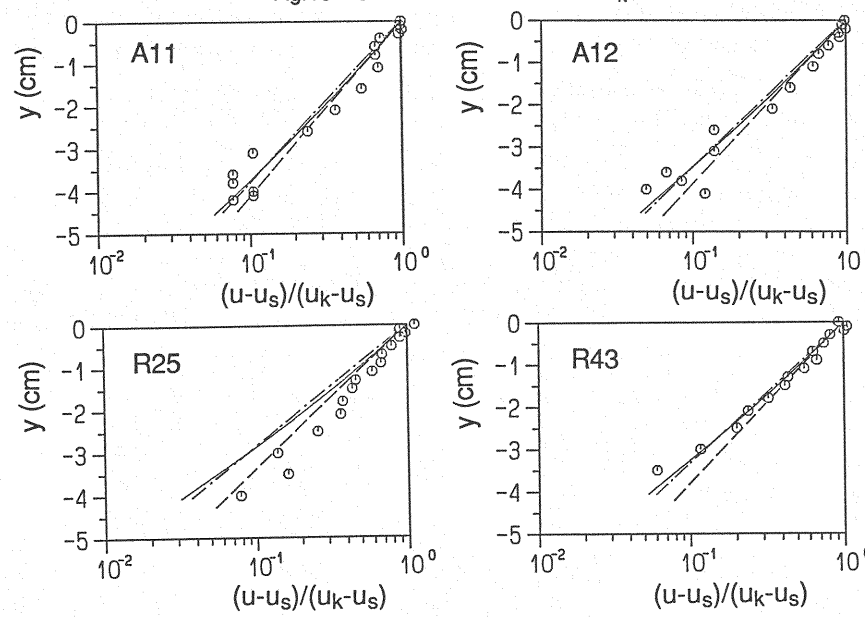

Fig.17 Velocity distribution in vegetation layer

Equation 13 suggests: $\beta=\alpha/2$ if $u_k>>u_s$, while $\beta=\alpha$ if $u_k\equiv u_s$. If Eq.10 is adopted for the relation between $\alpha\sqrt{sK}$ and hI/K, the relation between $\beta\sqrt{sK}$ and hI/K are calculated with the parameter $\gamma\equiv h/\sqrt{sK}$ as shown in Fig.18 with the data. This figure demonstrates that the method here predicts the velocity distribution in the vegetation layer or the parameter to represent it, β.

Since u_k is evaluated by Eq.12, Eq.9 determines the mixing length at $y=0$ (l_0). This evaluation of l_0 is supported by Fig.19. In Fig.19, l_0 is made dimensionless as $l_0/\sqrt{C_D\lambda h^3}$ and is plotted against hI/K, where the calculated curves are based on Eqs.8, 12, and 13.

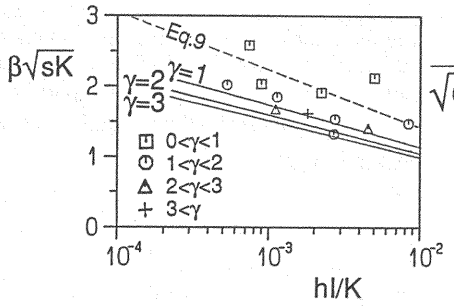

Fig.18 $\beta\sqrt{sK}$ vs hI/K

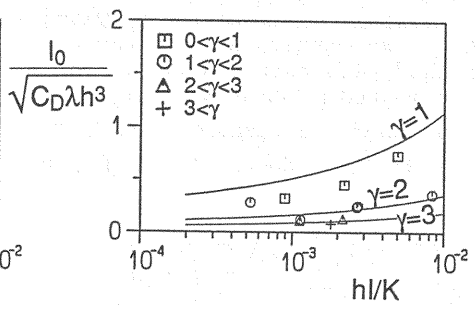

Fig.19 Evaluation of mixing length at the interface

Flow above the Vegetation Layer:

In the surface-flow region ($0<y<h$), the Reynolds-stress distribution is little affected by the vegetation, as in Eq.5. Assuming the mixing-length model, the velocity gradient in the surface-flow region is:

$$\frac{du}{dy}=\frac{u_{*k}}{l(y)}\sqrt{1-\frac{y}{h}} \qquad (0<y<h) \qquad (14)$$

The condition for the velocity gradient at $y=0$ is $l(+0)=l_0$, and the right-hand side is given by Eq.8. When the bed is not covered by vegetation, $\beta\to\infty$ and $l_0=0$. The distribution of mixing lengths for an open channel flow is often conveniently assumed as $l^*=\kappa\eta\sqrt{1-\eta}$ ($l^*\equiv l/h$; κ=Kármán constant; $\eta\equiv y/h$). For a surface flow over vegetation, it would be modified to:

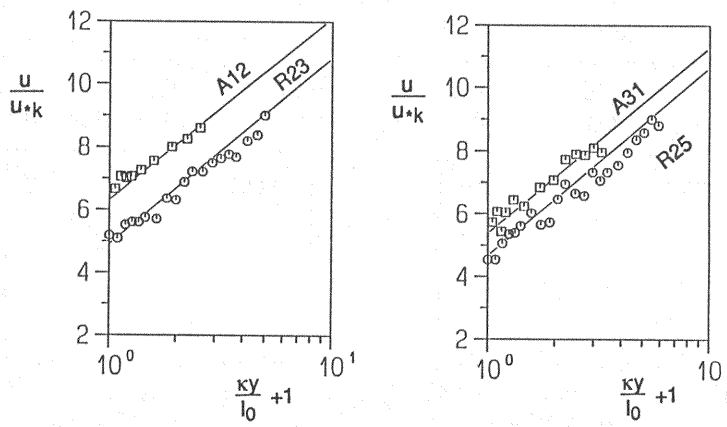

Fig.20 Velocity distribution above vegetation

$$l^*(\eta) = (\kappa\eta + l_0^*)\sqrt{1-\eta} \qquad (0<\eta<1) \qquad (15)$$

Christensen (1) also assumed a non-zero mixing length at the top of the vegetation without discussing its determination. The velocity profile in the surface-flow region over the vegetation layer then becomes:

$$\frac{u(\eta)}{u_{*k}} = \frac{1}{\kappa}\ln\left[\frac{\kappa\eta}{l_0^*}+1\right] + \frac{u_k}{u_{*k}} = \frac{1}{\kappa}\ln\left[\frac{\eta+\delta}{\delta}\right] + \frac{u_k}{u_{*k}} \qquad (0<\eta<1) \qquad (16)$$

in which $\delta \equiv l_0^*/\kappa$, δ may be termed the "shift of the theoretical wall" of the log-law, and δ or l_0^* is given as a function of β and u_k (they are expressed as functions of α by Eqs.13 and 12, respectively). Fig.20 demonstrates that the experimental profiles are well explained by Eq.16 with Eqs.12 and 13.

CONCLUSIONS

The results obtained in this investigation are summarized as follows:

(1) The turbulence characteristics of uniform flow in a vegetation-covered channel were investigated with vertical cylinders of the same diameter and height as simulated vegetation in the open channel bed. The turbulence characteristics in the free-surface flow region are little affected by the vegetation layer, while, the flow in the vegetation layer is strongly affected by faster surface flows.

(2) The effects may be summarized by noting the appearance of turbulent shear flows even in the vegetation layer. The profiles of the induced velocity and Reynolds-stress in the vegetation layer are roughly approximated by exponential functions, with parameters α and β, representing the turbulent flow structure in the vegetation layer with u_k the velocity at the interface. The β and u_k values also determine the boundary conditions for the velocity and velocity gradient at the interface between the vegetation and the surface-flow region.

(3) With the induced velocity profile in the vegetation layer approximated by an exponential function, a method to correct the energy slope, which is difficult to determine experimentally, is proposed. This correction results in a reduction in the scatter of the data, showing the relations among α, β, u_k, and the shear intensity of the surface flow at the top of the vegetation.

(4) An analytical model describing the turbulence structure in the vegetation layer, which leads to the relations among α, β, and u_k, was derived by assuming that the induced Reynolds-stress distributes exponentially in the vegetation layer. Thus, with α, a parameter of exponential distribution of induced Reynolds-stress, predicted with the hydraulic conditions and the properties of the vegetation, the flow structure in the vegetation layer and in the surface-flow region can be described analytically.

ACKNOWLEDGEMENTS

Laboratory experiments were conducted at Kyoto and Kanazawa Universities. Messrs. Yoshiyuki Iwata and Hisanobu Sato (Ministry of Construction) helped with the experiments at Kyoto University. We wish to thank Prof. Hiroji Nakagawa (Kyoto University) for encouragement and advice.

REFERENCES

1. Christensen, B.A. : Open channel and sheet flow over flexible roughness, *Proc. 24th IAHR Cong.*, Melbourne, Australia, Vol.1, pp.462-467, 1985.
2. Chu, Y. and L.W. Gelhar : Turbulent pipe flow with granular permeable boundaries, *Report*, Ralph Parsons Lab., M.I.T., No.148, 1972.
3. Fukuoka, S. and K. Fujita : Hydraulic effects of luxuriant vegetations on flood flow, *Report*, Public Works Res. Inst., Ministry of Construction, Vol.180, pp.129-192, 1990 (in Japanese).
4. Hino, M. and H. Utahara : Hydraulic characteristics of flow with water plants, *Proc. JSCE*, No.266, pp.87-94, 1977 (in Japanese).

5. Kouwen, N. and R.M. Li : Biomechanics of vegetative channel linings, *Jour. Hydraul. Div.*, ASCE, Vol.106, HY6, pp.1085-1103, 1980.
6. Kouwen, N. and T.E. Unny : Flexible roughness in open channels, *Jour. Hydraul. Div.*, ASCE, Vol.99, HY5, pp.713-728, 1973.
7. Kouwen, N., T.E. Unny and H.M. Hill : Flow retardance in vegetated channels, *Jour. Irri.& Drainage Div.*, ASCE, Vol.95, IR2, pp.329-342, 1969.
8. Murota, A. and T. Fukuhara : Experimental study on turbulent structure in open-channel flow with aquatic plants, *Proc. JSCE*, No.338, pp.97-103, 1983 (in Japanese).
9. Murota, A. and T. Fukuhara : Flow structure in a vegetated open channel, *Proc. 28th Japanese Conf. on Hydraul.*, JSCE, pp.225-231, 1984 (in Japanese).
10. Murota, A., T. Fukuhara and K. Murakoshi : Resistance characteristics of flow with water plants, *Proc. 29th Japanese Conf. on Hydraul.*, JSCE, pp.839-844, 1985 (in Japanese).
11. Nakagawa, H., T. Tsujimoto and Y. Shimizu : Open channel flow with water plants, *Proc. Hydraul. Engrg.*, JSCE, Vol.34, pp.475-480, 1990 (in Japanese).
12. Shen, H.W. : Flow resistance over short simulated vegetation and various tall vegetation groupings on flow resistance and sediment yield, *Environ. Impact on Rivers*, ed. by H.W. Shen, Chapt. 3, 51p., 1973.
13. Shimizu, Y., T. Tsujimoto, H. Nakagawa and T. Kitamura : Experimental study on flow over rigid vegetation simulated by cylinders with equi-spacing, *Proc. JSCE*, No.438/II-17, pp.31-40, 1991 (in Japanese).
14. Thom, A.S. and M.R. Raupach : Turbulence in and above plant canopies, *Ann. Rev. Fluid Mech.*, Vol.13, pp.97-129, 1981.
15. Tsujimoto, T. : Hydraulics of flow with vegetation in open channels, *Lecture Notes, 27th Summer Seminar on Hydraul. Engrg.*, Course A, JSCE, 91-A-5, pp.1-22, 1991 (in Japanese).
16. Tsujimoto, T. and T. Kitamura : Velocity profile in vegetated-bed channels, *KHL-Commun.*, Kanazawa Univ., No.1, pp.43-56, 1990.

APPENDIX - NOTATION

The following symbols are used in this paper:

C_D	= drag coefficient of model-plants;
D	= diameter of model-plants;
g	= gravity;
h	= water depthabove the vegetation (H-K);
H	= depth (from bottom to surface);
I	= energy gradient;
i_b	= bed slope;
K	= vegetation height;
l, l_0	= mixing length and value at y=0;
l^*	$\equiv l/h$ = dimensionless mixing length;
s	= distance between individual plants;
u	= local velocity;
U	= depth averaged velocity;
y	= vertical distance from the top of the vegetation layer;
y_0	= height where the Reynolds stress becomes zero in the vegetation layer;
u_k	= velocity at the interface between vegetation and surface-flow region;
u_s	= characteristic velocity of flow in vegetation layer given by Eq.1;
u_*	$= \sqrt{gHI} = \sqrt{\tau_0/\rho}$ = shear velocity;
u_{*k}	$= \sqrt{ghI} = \sqrt{\tau_k/\rho}$;

α, β = reciprocals of length for velocity and Reynolds-stress profiles in vegetation layer;

γ $\equiv h/\sqrt{sK}$;

δ $\equiv l_0^*/\kappa$;

κ = Kármán constant;

λ $\equiv D/s^2$ = projected area of vegetation to the flow per unit volume of water;

τ_0 = bed shear stress ($\equiv \rho g H I$);

τ_k = Reynolds stress at the top of vegetation;

τ_R = Reynolds stress; *and*

η $\equiv y/h$.

(Received December 24, 1991; revised march 26, 1992)